DOI: 10.1002/anie.200907088

Quantum Wires

Synthesis of Ideal AM-6 and Elucidation of V^{4+}-to-O Charge Transfer in Vanadate Quantum Wires**

*Shuvo Jit Datta and Kyung Byung Yoon**

The synthesis and characterization of one-dimensional (1D) semiconductor quantum-confined materials are important, since they have great potential as building blocks for nanoscale electronic devices and other applications.[1–9] Among the known 1D semiconductor materials, molecular wires or quantum wires[1–5] are the thinnest 1D quantum-confined materials. However, examples of such quantum wires are rare. Recently, we elucidated the interesting quantum-confinement properties of titanate (TiO_3^{2-}) quantum wire[10] regularly placed within a titanosilicate molecular sieve known as ETS-10.[11–13] It shows a length-dependent quantum-confinement effect even at length scales longer than 50 nm.[10] Its estimated effective reduced exciton mass along the wire μ_z is lower than $0.0006\,m_e$ (m_e = rest mass of electron), which is much lower than the lowest reported values (InSb: $0.014\,m_e$, single-walled carbon nanotubes (SWNT): $0.019\,m_e$) and indicate much higher exciton mobility along the quantum wire than in InSb and SWNTs. The nature of the electronic absorption of the titanate quantum wire was reportedly oxide-to-Ti^{IV} charge transfer or ligand-to-metal charge transfer (LMCT).[14–16] The stretching frequency of the titanate wire increases with increasing electron density of the wire.[14]

After elucidation of such important properties of titanate quantum wire, it would be of interest to determine the physicochemical properties of the closely related vanadate (VO_3^{2-}) quantum wire. In this regard, the discovery of vanadosilicate AM-6 by Rocha, Anderson, and co-workers in 1997[17] [designated AM-6-(RA)] is important, since it adopts the ETS-10 structure but with VO_3^{2-} quantum wires replacing TiO_3^{2-} quantum wires. Unfortunately, however, ETS-10 crystals were required as seeds to induce ETS-10 structure in the vanadosilicate. Accordingly, AM-6-(RA) inevitably contains ETS-10 crystals within AM-6. Thus, AM-6-(RA) should more strictly be defined as ETS-10 core/AM-6 shell. Furthermore, Lobo, Doren, and co-workers revealed that VO_3^{2-} quantum wires in AM-6-(RA) are composed of both V^{4+} and V^{5+}.[18–20] As a result, it is intrinsically impossible to elucidate the physicochemical properties of the pure $V^{IV}O_3^{2-}$ quantum wire. Furthermore, their procedure always simultaneously produces substantial amounts of quartz. Hence, methods to prepare ETS-10-free, pure AM-6 have long been awaited.

Twelve years after the report of AM-6-(RA), Sacco, Jr. and co-workers finally developed a method of synthesizing ETS-10-free AM-6.[21] However, they had to use tetramethylammonium ion (TMA^+) as structure-directing agent. Accordingly, this AM-6 contains TMA^+ ions within the channels. We designate this AM-6 as AM-6-(S)-TMA. We found that AM-6-(S)-TMA also contains both V^{4+} and V^{5+} (see below). Furthermore, the TMA^+ ions are tightly encapsulated within and hence completely block the silica channels. As a result, ion exchange of the pristine cations (Na^+ and K^+) with other cations is very difficult (see below), and makes it unsuitable for studying the physicochemical properties of the pure $V^{IV}O_3^{2-}$ quantum wire or pure V^{IV} vanadosilicate molecular sieve. Sacco, Jr. et al. removed the TMA^+ ions by treating AM-6-(S)-TMA with NH_3 gas for 3–4 h at 350-400 °C. These harsh conditions destroy all of the vanadate quantum wires, since they are not stable at temperatures higher than 180 °C (see below) under vacuum. We designate the NH_3-treated AM-6-(S)-TMA as AM-6-(S)-NH_3.

Thus, despite their great importance, no methods are available to synthesize ideal V^{IV} vanadosilicate AM-6 that has well-preserved $V^{IV}O_3^{2-}$ quantum wires and is free from ETS-10 cores and channel-blocking TMA^+ cations. Furthermore, the synthesis of AM-6-(RA) and AM-6-(S)-TMA usually requires three days or longer, and the vanadyl sulfate ($VOSO_4$) used as vanadium source is significantly more expensive ($>5\times$) than vanadium pentoxide. Therefore, the development of rapid and inexpensive synthetic methods to produce ideal V^{IV} AM-6 would be an important contribution to nanomaterials science and catalysis. We now report a rapid, seedless, template-free, and inexpensive synthesis of pure V^{IV} AM-6 [AM-6-(Y)] that uses V_2O_5 as vanadium source and that, in the case of $V^{IV}O_3^{2-}$ quantum wire, the nature of the intense electronic absorption in the 3.0–5.5 eV region is V^{4+}-to-O^{2-} CT or metal-to-ligand CT (MLCT) as opposed to the previous assignments[18] and in contrast to TiO_3^{2-} quantum wire.

AM-6-(Y) was readily obtained from a gel composed of Na_2SiO_3, V_2O_5, H_2SO_4, KOH, ethanol, and water (Supporting Information SI 1), despite the fact that V_2O_5 (V^{5+} source) was used instead of $VOSO_4$ (V^{4+} source). For comparison we also prepared AM-6-(RA), AM-6-(S)-TMA, and AM-6-(S)-NH_3

[*] S. J. Datta, Prof. Dr. K. B. Yoon
Korea Center for Artificial Photosynthesis
Center for Microcrystal Assembly
and
Department of Chemistry, Sogang University
Seoul 121-742 (Korea)
Fax: (+82) 2-706-4269
E-mail: yoonkb@sogang.ac.kr

[**] We thank the Ministry of Education, Science, and Technology (MEST) of the Korean Government and the National Research Foundation of Korea for supporting this work through the Korea Center for Artificial Photosynthesis (KCAP) located in Sogang University (NRF-2009-C1AAA001-2009-0093879) and Acceleration Research.

Supporting information for this article is available on the WWW under http://dx.doi.org/10.1002/anie.200907088.

according to the reported procedures. The X-ray powder diffraction pattern of AM-6-(Y) confirmed its ETS-10 structure and showed that, unlike AM-6-(RA), it is not contaminated with impurities such as quartz (SI 2). The scanning electron microscopy (SEM) image of AM-6-(Y) crystals showed that the crystals adopt the typical truncated octahedral shape with average *a*/*c* ratio of 1.38, and their surfaces are very smooth (Figure 1). In contrast, the typical *a*/*c* ratio of AM-6-(RA) is 0.8 and many crystals have rough broken faces. The crystal shapes of AM-6-(S)-TMA are irregular and the surfaces are very rough. The transmission electron microscopy (TEM) image of AM-6-(Y), shown in Figure 2, further confirmed its AM-6 structure and revealed that it has defects and is a mixture of polymorphs A and B.

The average yields of AM-6-(Y), AM-6-(RA), and AM-6-(S)-TMA were 84, 49, and 48 % (with respect to the amount of vanadium), respectively, that is, the synthetic procedure for AM-6-(Y) is much more economical, not only because it uses much cheaper V_2O_5 as vanadium source, but also because of its much higher yield. Furthermore, the required reaction time was only 20 h at 220 °C, which is much shorter than the typical reaction times for the synthesis of AM-6-(RA) and AM-6-(S)-TMA (> 3 d).

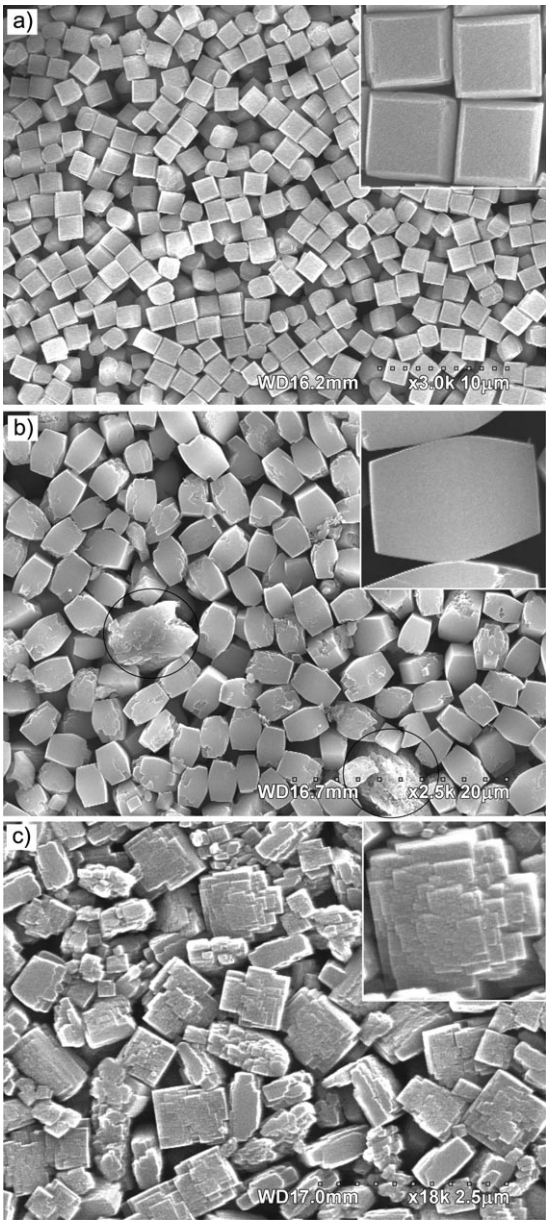

Figure 1. SEM images of a) AM-6-(Y), b) AM-6-(RA), and c) AM-6-(S)-TMA crystals with average lengths along the [110] direction of 1.5, 3, and 0.3–1 μm, respectively. Insets show higher magnification images. The circles in (b) indicate quartz impurities.

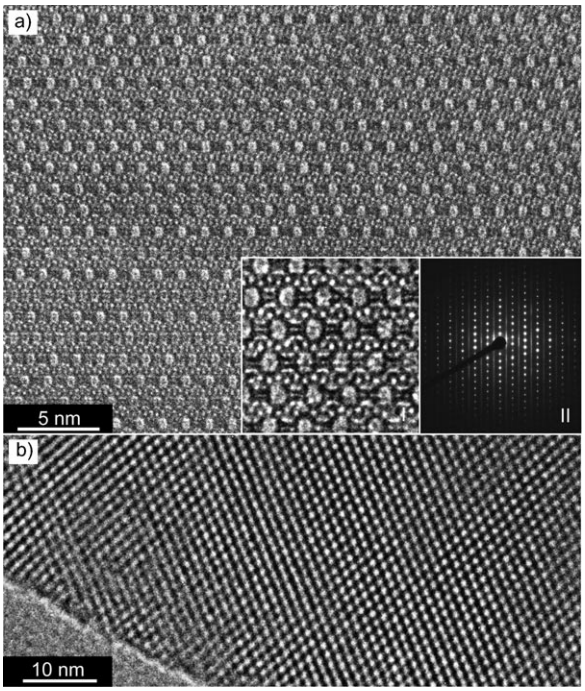

Figure 2. TEM images of an AM-6-(Y) crystal along the a) channel [110] and b) [001] directions. Inset I in (a): the channel direction image at a higher magnification. Inset II in (a): selected-area electron diffraction pattern along the [110] direction.

Thermogravimetric analysis (TGA) of pristine AM-6 samples with air as eluting gas (SI 3) revealed that water loss continues up to 500 °C and that AM-6-(S)-TMA indeed contains an organic template. In the case of AM-6-(RA), the amount of water lost in the temperature range 100–250 °C is larger than that of AM-6-(Y), and its TGA curve resembles that of ETS-10. This is indirect evidence for the existence of ETS-10 core in the former.

The BET surface areas of pristine AM-6-(Y), AM-6-(RA), AM-6-(S)-TMA, and AM-6-(S)-NH_3, measured by nitrogen adsorption (SI 4), are 395, 417, 81, and 296 $m^2 g^{-1}$, respectively. The very small surface area of AM-6-(S)-TMA indicates that most of the pores are blocked by TMA^+ ions. The significantly smaller surface area of AM-6-(S)-NH_3 compared to AM-6-(Y) and AM-6-(RA) further indicates that the structures are partially damaged after TMA^+ removal with NH_3. The N_2 adsorption isotherm of AM-6-(RA) further shows the presence of mesopores in the sample. The

mesopores are likely formed between the ETS-10 core and AM-6 shell through facile disconnection of -Ti-O-Ti-O-V-O-V- quantum wires into -Ti-O-Ti-OH and HO-V-O-V- chains at the core/shell interfaces. The existence of such mesopores seems to be responsible for the slightly higher surface area of AM-6-(RA) compared to AM-6-(Y).

Ion exchange of various cations (K^+, Na^+, Ba^{2+}, Sr^{2+}, Ca^{2+}, Mg^{2+}, Pb^{2+}, Cd^{2+}, and Zn^{2+}) into AM-6-(Y), AM-6-(RA), AM-6-(S)-TMA, and AM-6-(S)-NH_3 was carried out at room temperature with 1M solutions of metal salts for 150 min and repeated three times. The resulting degrees of ion exchange were 80–99, 70–94, 6–26, and 60–77% for AM-6-(Y), AM-6-(RA), AM-6-(S)-TMA, and AM-6-(S)-NH_3, respectively (SI 5). Thus, the degree of ion exchange increases in the order AM-6-(Y) > AM-6-(RA) > AM-6-(S)-NH_3 ≫ AM-6-(S)-TMA. This result shows that the TMA^+ ions in AM-6-(S)-TMA significantly hamper ion exchange with metal cations by blocking the channels, and removal of TMA^+ ions by treatment with hot NH_3 does not produce undamaged AM-6.

The Raman spectra of pristine ETS-10, AM-6-(RA), AM-6-(S)-TMA, AM-6-(S)-NH_3, and AM-6-(Y) are compared in Figure 3. AM-6-(Y) showed the longitudinal V-O-V stretching vibration at 871 cm^{-1}, which is slightly blueshifted with respect to those of AM-6-(RA) and AM-6-(S)-TMA, which appear at 869 cm^{-1} (SI 6). The slight blueshift is attributed to the higher K^+/Na^+ ratio of AM-6-(Y) compared to AM-6-(RA) and AM-6-(S)-TMA[14] (SI 7). The Raman spectrum of AM-6-(RA) always shows the Ti-O-Ti longitudinal stretching vibration at 724 cm^{-1} in addition to that of V-O-V. The Raman spectrum of AM-6-(S)-TMA showed an additional weak Raman band due to TMA^+ at 756 cm^{-1} (SI 8). Unlike other AM-6 samples, AM-6-(S)-NH_3 did not show the V-O-V stretching vibration, that is, all V-O-V quantum wires were destroyed during the process of TMA^+ removal. We found that NH_3 treatment even for 45 min at 300 °C (instead of 3 h at 350 °C) is enough to destroy all V-O-V quantum wires (SI 9). A thermal stability test under vacuum revealed that the V-O-V quantum wire starts decomposing at 180 °C (Figure 3b), that is, the V-O-V quantum wire in AM-6 is thermally less stable than Ti-O-Ti quantum wire in ETS-10, which starts decomposing at 250 °C.[14] The narrowest peak width (full width at half-maximum (FWHM): 10 cm^{-1}) further supports that the V-O-V chain in AM-6-(Y) has the highest quality.

Based on the unit cell formula ($M^I_2VSi_5O_{13}\cdot x\,H_2O$), the oxidation state of each V atom in ideal AM-6 must be +4. This means that each vanadium atom should have one unpaired electron, and hence the theoretical atomic magnetic moment μ should be 1.73 BM. The measured μ of AM-6-(Y) is 1.76 BM, while those of AM-6-(RA), AM-6-(S)-TMA, and AM-6-(S)-NH_3 are 1.47, 1.52, and 1.30 BM, respectively (Figure 3c). This result also indicates that while most of the vanadium atoms in AM-6-(Y) exist in the +4 oxidation state, substantial fractions of the vanadium atoms in other AM-6 samples exist in the +5 oxidation state, consistent with the literature report.[18–20]

The ESR spectra of AM-6-(Y), AM-6-(RA), AM-6-(S)-TMA, and AM-6-(S)-NH_3 showed sharp signals of V^{4+} with g values of 1.9592, 1.9595, 1.9593, and 1.9598 and ΔH_{pp} values of 51, 57, 57, 66 G, respectively (SI 10). The relative ESR intensities of AM-6-(Y), AM-6-(RA), AM-6-(S)-TMA, and AM-6-(S)-NH_3 were 1, 0.79, 0.81, and 0.69, respectively, for the same loaded amount (0.4 g), that is the intensity of V^{4+} decreases in the order AM-6-(Y) > AM-6-(S)-TMA > AM-6-(RA) > AM-6-(S)-NH_3. The observed ESR intensity showed a linear relationship with μ (SI 11A), that is, both methods are useful for comparing the relative amounts of V^{4+} centers. Interestingly, the negative linear relationship between the μ value (amount of V^{4+} centers) and ΔH_{pp} (ESR peak width) shown in SI 11B indicates that the degree of interaction between V^{4+} and V^{5+} increases with increasing amount of V^{5+} or decreasing amount of V^{4+}.

The TGA data of the pristine AM-6 samples (SI 3) further revealed a weight increase beginning between 470 and 520 °C. Since ETS-10 does not undergo weight increase, the above increase is assigned to oxidation of V^{4+} to V^{5+}. The weight increases (theoretical values in parentheses) were 1.30 (1.75), 1.15 (1.80), 0.89 (1.83), and 1.20% (1.83%), respectively. The reason for the discrepancy between experimental and calculated values is that the weight increase due to oxidation of V^{4+}, which begins at 470 °C, overlaps with that due to dehydration, which continues up to about 500 °C.

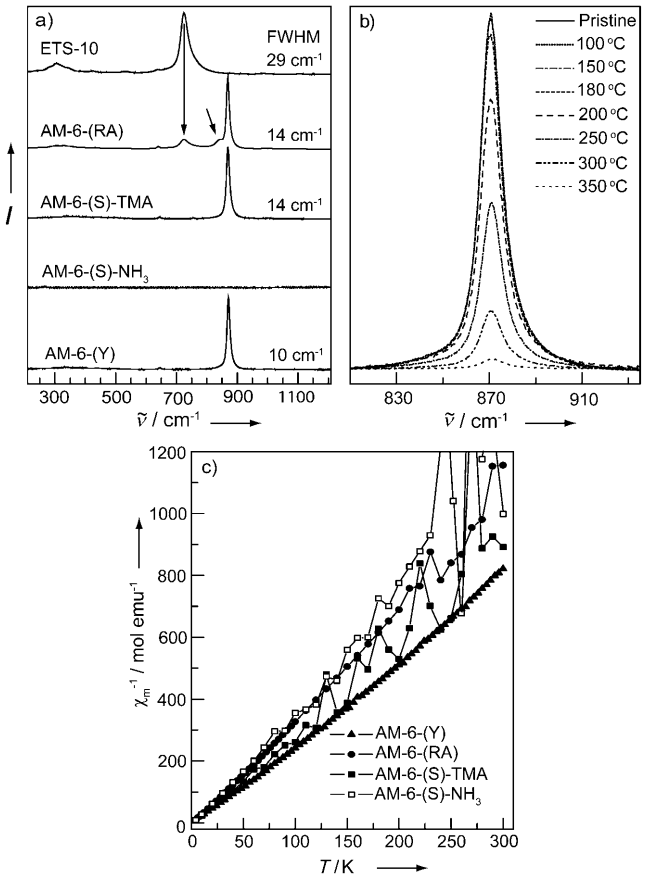

Figure 3. a) Raman spectra of ETS-10, AM-6-(RA), AM-6-(S)-TMA, AM-6-(S)-NH_3, and AM-6-(Y). b) Progressive intensity decrease of the longitudinal V-O-V Raman stretching band with increasing temperature under vacuum. c) Reciprocal magnetic susceptibility $1/\chi_M$ versus temperature for various AM-6 samples.

Thus, the μ values, ESR spectra, and TGA data give insights into the absolute or relative amounts of V^{4+} centers in AM-6 samples. However, they do not reflect the purity of the V-O-V chain, because AM-6-(S)-NH_3 also showed a substantial μ value, a strong ESR signal, and large weight increase due to the oxidation of V^{4+} to V^{5+} despite the fact that its Raman spectrum shows that the V-O-V chains were completely destroyed (see above).

The above results demonstrate that AM-6-(Y) is indeed ideal in various respects: smooth crystal surfaces, no ETS-10 seeds, no pore-blocking TMA^+ ions, all V atoms in +4 oxidation state, and high-quality $V^{IV}O_3^{2-}$ quantum wires. This gave us the unique opportunity to study the nature of the electronic transitions of the $V^{IV}O_3^{2-}$ quantum wire. The UV/Vis spectra of the four pristine AM-6 samples and ETS-10 are compared in Figure 4a. Each spectrum is composed of a strong absorption band in the UV region and weaker absorption bands in the visible and near-IR regions. The absorption maxima (λ_{max}) in the UV region are 218, 219, 247, 280, and 285 nm for AM-6-(S)-TMA, AM-6-(S)-NH_3, AM-6-(Y), AM-6-(RA), and ETS-10, respectively. Detailed spectral analyses will be the subject of a future study. Nevertheless, comparison of the UV-region spectra again shows that AM-6-(RA) contains ETS-10 core. The large redshift of the tail absorption on going from AM-6-(S)-TMA to AM-6-(S)-NH_3 indicates that the VO_3^{2-} quantum wires are damaged during removal of TMA^+ ions with hot NH_3.

The electronic absorption spectra of a series of AM-6-(Y) exchanged with K^+, Na^+, Ba^{2+}, Sr^{2+}, Ca^{2+}, Mg^{2+}, Pb^{2+}, Cd^{2+}, and Zn^{2+}, respectively, in the dry state (see SI 5 for the cation compositions) revealed that λ_{max} of the UV-region absorption band and the band-gap energy E_g, estimated from the inflection point of each absorption spectrum, are progressively redshifted with increasing electronegativity[22] of the countercation (Figure 4b). Furthermore, λ_{max} and E_g showed linear relationships with the Sanderson partial charge of the framework oxygen atoms $\delta(O_f)$ (Figure 4c, SI 12). This reveals that the UV-region band is due to V^{4+}-to-O^{2-} CT or MLCT as opposed to the previous assignment (LMCT)[18] and in contrast to titanate quantum wire.[14–16] We believe that this is the first demonstration of MLCT in an oxide molecular sieve. AM-6-(RA) and AM-6-(S)-NH_3 also showed the same trend (SI 13). However, for the aforementioned reasons they are unsuitable for elucidating the physical properties of the vanadate quantum wire (see above).

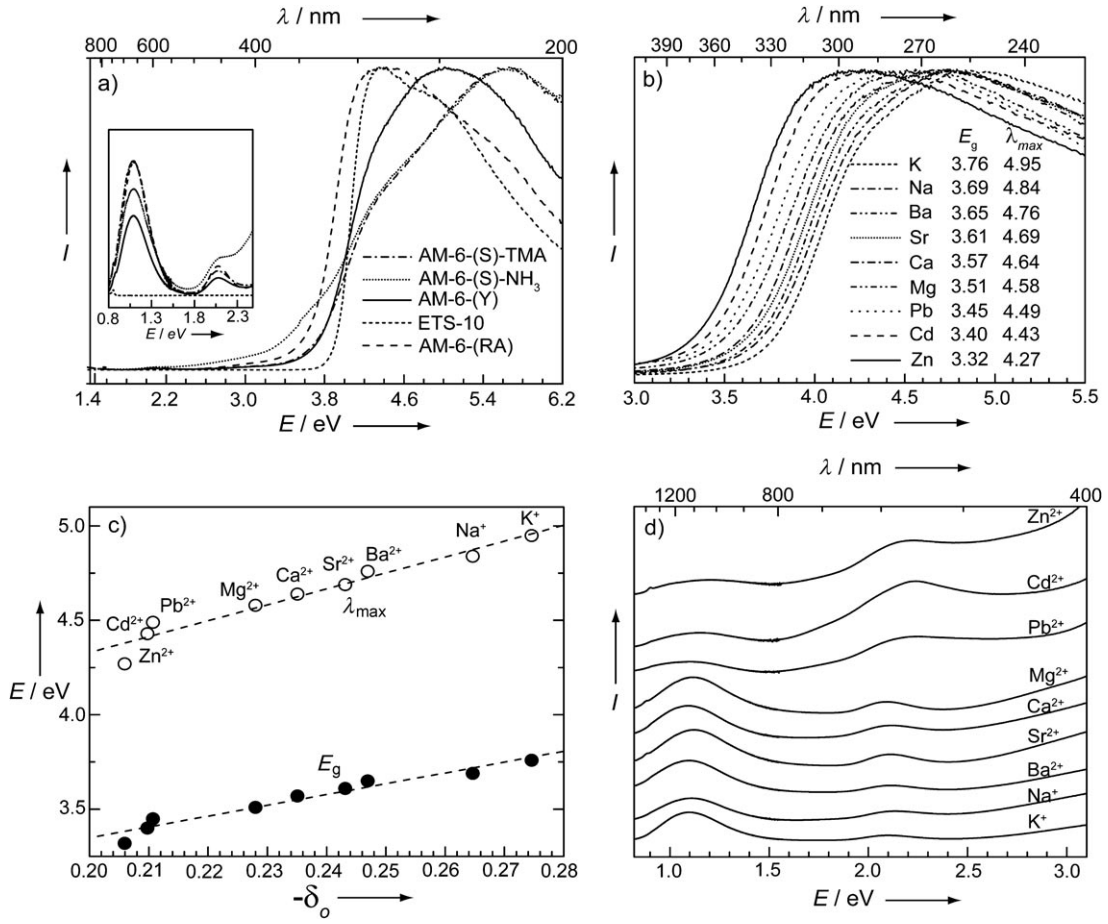

Figure 4. Diffuse-reflectance UV/Vis spectra of a) pristine AM-6 samples in the 1.4–6.2 eV region and b) AM-6-(Y) samples exchanged with various cations in the 3.0–5.5 eV region. c) Linear relationships between the absorption maximum λ_{max} and the Sanderson partial negative charge $-\delta_o$, and between the band-gap energy E_g and $-\delta_o$. d) Diffuse-reflectance UV/Vis spectra of AM-6-(Y) samples exchanged with various cations in the 0.8–3.1 eV region.

Unlike the UV-region band, the visible (2.1 eV) and near-IR (1.1 eV) bands did not shift in positions upon varying the countercation, except for Pb^{2+}, Cd^{2+}, and Zn^{2+} (Figure 4d, SI 14). This result indicates that they arise from d–d transitions of V^{4+}, as opposed to the previous assignment (LMCT).[18] If we assume that the -O-V^{4+}(O)$_4$-O- structure adopts the flattened (*z*-in) octahedral structure like ETS-10,[16,23,24] the transitions at 1.1 and 2.1 eV are likely to arise from the $d_{xy} \rightarrow d_{x^2-y^2}$ and $d_{xy} \rightarrow d_{z^2}$ transitions, respectively.

The synthesis of AM-6-(Y) from V_2O_5 is noteworthy in the sense that the oxidation state of V in V_2O_5 is 5+ while the oxidation states of all V atoms in AM-6-(Y) are 4+. Evidently, the added ethanol acts as a one-electron reducing agent during the synthesis. Various other alcohols are also effective, and the details of the effect of other alcohols on the synthesis will be reported elsewhere. We believe that this work will accelerate the application of pure AM-6 for various purposes and to elucidate various novel physicochemical properties of the $V^{IV}O_3^{2-}$ quantum wire. It will also lead to insights into the synthesis and chemistry of vanadosilicate molecular sieves.[25–29]

Received: December 16, 2009
Published online: June 8, 2010

Keywords: charge transfer · quantum wires · vanadium · vanadosilicates · zeolite analogues

[1] L. Venkataraman, C. M. Lieber, *Phys. Rev. Lett.* **1999**, *83*, 5334–5337.
[2] M. Ouyang, J.-L. Huang, C. M. Lieber, *Acc. Chem. Res.* **2002**, *35*, 1018–1025.
[3] J. H. Golden, F. J. DiSalvo, J. M. J. Fréchet, J. Silcox, M. Thomas, J. Elman, *Science* **1996**, *273*, 782–784.
[4] J. H. Golden, H. Deng, F. J. DiSalvo, J. M. J. Fréchet, P. M. Thompson, *Science* **1995**, *268*, 1463–1466.
[5] Y. Xia, P. Yang, Y. Sun, Y. Wu, B. Mayers, B. Gates, Y. Yin, F. Kim, H. Yan, *Adv. Mater.* **2003**, *15*, 353–389.
[6] S. Kan, T. Mokari, E. Rothenberg, U. Banin, *Nat. Mater.* **2003**, *2*, 155–158.
[7] L.-S. Li, J. Hu, W. Yang, A. P. Alivisatos, *Nano Lett.* **2001**, *1*, 349–351.
[8] S. P. Ahrenkiel, O. I. Miedaner, C. J. Curtis, J. M. Nedeljković, A. J. Nozic, *Nano Lett.* **2003**, *3*, 833–837.
[9] H. Yu, J. Li, R. A. Loomis, L.-W. Wang, W. E. Buhro, *Nat. Mater.* **2003**, *2*, 517–520.
[10] N. C. Jeong, M. H. Lee, K. B. Yoon, *Angew. Chem.* **2007**, *119*, 5972–5976; *Angew. Chem. Int. Ed.* **2007**, *46*, 5868–5872.
[11] S. M. Kuznicki, US 4853202, **1989**.
[12] M. W. Anderson, O. Terasaki, T. Ohsuna, A. Philippou, S. P. MacKay, A. Ferreira, J. Rocha, S. Lidin, *Nature* **1994**, *367*, 347–351.
[13] M. W. Anderson, O. Terasaki, T. Ohsuna, P. J. O. Malley, A. Philippou, S. P. MacKay, A. Ferreira, J. Rocha, S. Lidin, *Philos. Mag. B* **1995**, *71*, 813–841.
[14] N. C. Jeong, Y. J. Lee, J.-H. Park, H. Lim, C.-H. Shin, H. Cheong, K. B. Yoon, *J. Am. Chem. Soc.* **2009**, *131*, 13080–13092.
[15] E. Borello, C. Lamberti, S. Bordiga, A. Zecchina, C. O. Areán, *Appl. Phys. Lett.* **1997**, *71*, 2319–2321.
[16] A. Damin, F. X. L. Xamena, C. Lamberti, B. Civalleri, C. M. Z. Wilson, A. Zecchina, *J. Phys. Chem. B* **2004**, *108*, 1328–1336.
[17] J. Rocha, P. Brandao, Z. Lin, M. W. Anderson, V. Alfredsson, O. Terasaki, *Angew. Chem.* **1997**, *109*, 134–136; *Angew. Chem. Int. Ed. Engl.* **1997**, *36*, 100–102.
[18] A. M. Shough, R. F. Lobo, D. J. Doren, *Phys. Chem. Chem. Phys.* **2007**, *9*, 5096–5104.
[19] M. J. Nash, S. Rykov, R. F. Lobo, D. J. Doren, I. Wachs, *J. Phys. Chem. C* **2007**, *111*, 7029–7037.
[20] A. M. Shough, D. J. Doren, M. Nash, R. F. Lobo, *J. Phys. Chem. C* **2007**, *111*, 1776–1782.
[21] M. N. Ismail, N. D. Fraiman, D. M. C. Jr, G. Gursoy, E. Viveiros, O. Ozkanat, J. Ji, R. J. Willey, J. Warzywoda, A. Sacco, Jr., *Microporous Mesoporous Mater.* **2009**, *120*, 454–459.
[22] The Sanderson electronegativities of the cations are K^+: 0.445, Na^+: 0.560, Ba^{2+}: 0.651, Sr^{2+}: 0.721, Ca^{2+}: 0.946, Mg^{2+}: 1.318, Pb^{2+}: 1.900, Cd^{2+}: 1.978, and Zn^{2+}: 2.223. R. T. Sanderson, *J. Am. Chem. Soc.* **1983**, *105*, 2259–2261.
[23] X. Wang, A. J. Jacobson, *Chem. Commun.* **1999**, 973–974.
[24] C. Prestipino, P. L. Solari, C. Lamberti, *J. Phys. Chem. B* **2005**, *109*, 13132–13137.
[25] X. Wang, L. Liu, A. J. Jacobson, *Angew. Chem.* **2003**, *115*, 2090–2093; *Angew. Chem. Int. Ed.* **2003**, *42*, 2044–2047.
[26] X. Wang, L. Liu, A. J. Jacobson, *J. Am. Chem. Soc.* **2002**, *124*, 7812–7820.
[27] X. Wang, L. Liu, A. J. Jacobson, *Angew. Chem.* **2001**, *113*, 2232–2234; *Angew. Chem. Int. Ed.* **2001**, *40*, 2174–2176.
[28] P. Brandão, A. Philippou, N. Hanif, P. R. -Claro, A. Ferreira, M. W. Anderson, J. Rocha, *Chem. Mater.* **2002**, *14*, 1053–1057.
[29] C.-Y. Li, C.-Y. Hsieh, H.-M. Lin, H.-M. Kao, K. W. Lii, *Inorg. Chem.* **2002**, *41*, 4206–4210.

